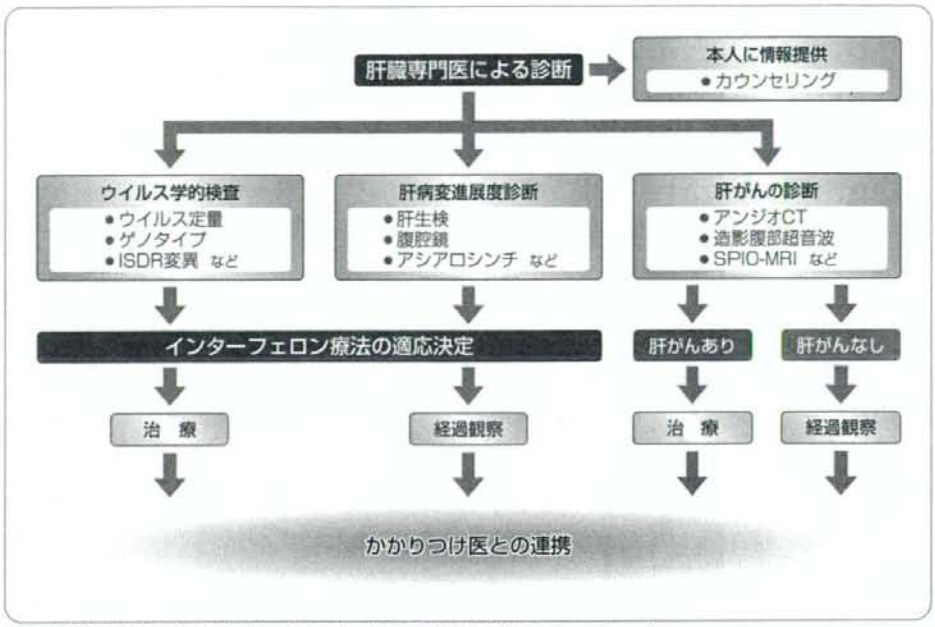

図2　検診で発見されたC型肝炎ウイルスキャリアのその後の経過のフローチャート

ととした．専門医に紹介する基準は，ALT 30 IU/mL以上，血小板15万/mL以下，あるいは肝腫瘍性病変を認める場合である．専門医レベルでは，ウイルス学的検査や画像診断による精査を行い，インターフェロン療法の適応の有無を評価し，適応があれば治療導入，なければ経過観察とした(図2)．

肝炎経過観察用のパスでは，①通常のC型慢性肝炎患者用のパスと，②ALT持続正常HCVキャリアに対する連携パスも作成した．とくに，ALT持続正常HCVキャリアに対する診療ガイドラインは厚生労働省の研究班で明示されているためこれを厳密に遵守する必要がある．具体的には，ALT31 IU/mL以上は基本的には慢性C型肝炎に準じて治療をすることとし，ALT30 IU/mL以下でも血小板が15万/μL以下であれば，専門医による精査が必要であり線維化がF2以上であれば治療が必要である．また，線維化が軽度であったり，血小板が15万/μL以上であっても放置は不可で2～4ヵ月ごとのフォローアップが必要であり，経過観察により治療適応の有無を再検討したり，肝がんの早期発見を行う必要がある．

V　肝がん治療後の連携パス

肝がんでは肝硬変を合併することが多いため，肝がん治療後の肝硬変の合併症を治療するための連携が必要である．DPC対象の急性期病院ではすべてを入院で行うことが困難であるため，地域の病院との間で病病連携パスを作成し，これを用いて肝がん治療後の肝硬変の合併症対策を行っている(図1)．

さらに肝がんをRFAなどによって根治できた場

図3 肝がん治療後の再発の早期発見のための医療連携パス

肝臓癌スクリーニング用 連携クリニカルパス(1)
様 年 月 日生 男・女

基本情報	年齢 歳	身長 cm	ゲノタイプ 型	AFP L3	肝組織：A F(年 月 日)
	BMI	体重 kg	AFP	PIVKA Ⅱ	腹腔鏡：

ID:

武蔵野赤十字病院消化器科：

紹介医：

疾患	合併症	ゴール設定	基本ルール	肉眼的stage	Child-Pugh	前回治療
□C型慢性肝炎 □ALT持続陽性HCVキャリア □代償性肝硬変 □非代償性肝硬変 □HCC □CCC	□食道静脈瘤L F C RC Lg □糖尿病 □高血圧 □高脂血症 □	□ALT正常化 □肝癌がない □肝不全がない	網掛けは武蔵野赤十字病院で検査 白抜きはかかりつけ医で検査 検査・診察を実施し問題なければ○をつける ▲記号がついたら要注意 著しい異常は× ×記号がついたら武蔵野赤十字病院を受診	□stage Ⅰ □stage Ⅱ □stage Ⅲ □stage *IV* □	□A □B □C	□ラジオ波 □エタノール局中 □肝動脈塞栓 □肝動注 □

	日付			基準・記号など	診療週数 0	4	8	12	16	20	24	28	32	36	40	44	48	52	56	60	64	68	72	76	80	84	88	92	96
	武蔵野赤十字病院で診察・検査				●			●			●			●			●			●			●			●			●
	連携かかりつけ医で診察・検査					○	○		○	○		○	○		○	○		○	○		○			○	○		○	○	
タスク	検査	血算	WBC Hb 血小板	正常値は○ 上昇は▲または× 低下は▲または× 血小板15以下は紹介		この間に1回検査			この間に1回検査			この間に1回検査			この間に1回検査			この間に1回検査			この間に1回検査			この間に1回検査		
		肝機能検査	Alb AST ALT T.Bil	正常値は○ ALT31以上× （日赤に紹介）																							
			HCVコア蛋白 HCVRNA定量	いずれか1項目を検査																							
			プロトロンビン時間	正常値は○																							
			ヘパプラスチン	低下は▲または×																							
	肝癌スク		AFP	正常値は○																							
			PIVKA-Ⅱ	上昇は▲または×																							
		診断画像	超音波 ダイナミックCT ダイナミックMRI	いずれか1つを検査 SOLありは×																							
	診察		下腿浮腫 腹水 黄疸 肝性脳症 便秘	症状有りは▲または×																							
	内服		ウルソ 肝庇護薬 BCAA製剤	投与は○																							
	注射・点滴		強ミノC IFN	投与は○																							

アウトカム			
	患者状態		肝不全と肝癌がない
	知識・教育		C型肝炎の病態を理解し通院することができる 肝硬変への進展・肝発癌のリスクを理解している 日常生活の注意点が理解できている
	合併症		①混合型クリオグロブリン血症 ②B細胞性非ホジキンリンパ腫 ③単クローン性ガンマグロブリン血症 ④晩発性皮膚ポルフィリン症 ⑤扁平苔癬（口腔，四肢など） ⑥メサンギウム増殖性糸球体腎炎 ⑦心筋炎 ⑧膜性増殖性糸球体腎炎 ⑨膜性腎症 ⑩自己免疫性甲状腺炎 ⑪自己免疫性血小板減少性紫斑病 ⑫Sjogren症候群 ⑬ぶどう膜炎，強膜炎 ⑭特発性肺線維症 ⑮肝不全 ⑯腹水 ⑰黄疸 ⑱肝性脳症 ⑲食道静脈瘤 ⑳

合でもC型肝炎ウイルス感染が見られる場合には，残肝に年率20%以上の割合で再発が見られる．したがって**再発の早期発見**とその防止のための連携パスが必要となる．

具体的には，肝がん治療後には3ヵ月に1回の腹部超音波と6ヵ月に1回の造影CTスキャンを行う（図3）．診療所では施行できない場合には専門医に紹介してもらい，そこで画像診断を行う．さらに画像診断のみでは発見できない肝がんを見落とさないために，腫瘍マーカーを毎月測定し，もし上昇した場合には専門医で再発の早期発見のための検査を行う．

また，**再発を抑止していく対策**も重要である．ASL・ALT値が高い場合に再発が高頻度で見られるため，強力ネオミノファーゲンシー®の静注やウルソデオキシコール酸内服によってALT値を低下させ，再発抑止を行っていく．さらにアルブミン値が低い場合に再発が多く，また肝硬変の進展を防止する目的でバリン・ロイシン・イソロイシンの分岐鎖アミノ酸（BCAA）の合剤を内服して治療を行っていくことも重要である．さらに，ALT値の低下が十分でない場合には，少量のインターフェロンの注射を行い再発の防止や肝硬変の進展抑止を図っていく．

これらの治療は，すべてを専門医で施行することが困難なことが多く，地域医療連携で行ったほうが効率的に施行できる．そこで連携パスが有用となってくる．

Ⅵ 地域医療連携パスを効率的に運用するために

厚生労働省は地域における肝疾患診療拠点院構想の構築に乗り出している．そのため，当地域パスをさらに普及させ定着させる必要がある．したがって，今後もその活動を地域肝炎研究会などを通じて各医師会とともに展開していかなければならない．現在は，まだ少人数のワーキンググループを核としたパスの運用が中心であるのが実態である．しかし，このワーキンググループ内で運用して実際に見えてくる具体的な問題点について，さらに吟味し改良を加えて地域に浸透するものに仕上げて行きたいと考えている．

また，実際の運用方法をめぐっては紙ベースの運用では限界があるとの意見も出ている．患者一人ひとりの診療情報を連携医療機関でリアルタイムに共有し，「2人の主治医」がそのデータを前にディスカッションするためには，コンピュータ・ネットワークを利用したIT化が欠かせない．現時点では，患者情報保護などの観点から障害も多いが，今後IT化は積極的に推進して行く重要課題であると考えられる．

医療連携のポイントは，①エビデンスに基づく質の高いプロトコルを地域のコンセンサスとして共有すること，②患者の視点に立つこと，③患者および連携医療機関の利便性を重視すること，④専門医療機関とかかりつけ医が同じ目線でディスカッションできることなどがあげられる．肝炎診療は，専門医からかかりつけ医への一方的な治療方針の提示ではなく，専門医もかかりつけ医も，同じ目線で治療にのぞみ，地域全体でレベルアップを図っていく姿勢が欠かせない．今後は連携パスを有効活用し，患者がどこでも安心して医療が受けられるよう，質の高い一定水準の医療を提受けられるよう，質の高い一定水準の医療を提供していく必要がある．

Original Paper

Therapeutic Effect of TAE Can be Predicted by Abdominal-enhanced CT Findings in HCC

Shinjiro Kobayahsi MD, Satoshi Katagiri MD, Shyunichi Ariizumi MD, Masakazu Yamamoto PhD
Department of Surgery, Institute of Gastroenterology, Tokyo Women's Medical University, Tokyo, Japan
Corresponding Author: Shinjiro Kobayashi, MD, Department of Surgery, Institute of Gastroenterology
Tokyo Women's Medical University, 8-1, Kawada-cho, Shinjuku-ku, Tokyo 162-8666, Japan,
Tel: +81 3 3353 8111, Fax: +81 3 5269 7507, E-mail: gxptd195@ybb.ne.jp

ABSTRACT

Background/Aims: In order to improve the therapeutic efficacy of transcatheter arterial embolization (TAE) in hepatocellular carcinoma (HCC), the relationship between CT findings and antitumor efficacy was studied.

Methodology: The therapeutic effect on CT 1 year after TAE was respectively studied for 100 nodules of HCC where TAE was performed. The pre-treatment abdominal CT findings were classified, and the therapeutic effect was compared with regard to these attributes.

Results: Tumors determined to have no recurrence at the treated site (defined as "complete necrosis") accounted for 58% overall. The percentage of "complete necrosis" in pre-TAE CT findings by type showed that 1) in terms of tumor shape, 73.4% were smooth type, 34.5% irregular type, and 0% invasive type (p=0.0003), 2) in terms of the presence of corona nodules, nodules where "complete necrosis" was achieved were corona-positive in 67.7% and corona-negative in 37.1% (p=0.003), 3) in terms of tumor size, 68.3% of tumors were smaller than 3.0cm and 28.6% were larger than 3.1cm, 4) in terms of location, 64.6% of tumors were in a peripheral location and 28.6% in a central location (p=0.006).

Conclusions: The therapeutic effect of TAE is improved by adequate diagnosis of the tumor characteristics found on pre-treatment CT.

KEY WORDS: Hepatocellular carcinoma; Transcatheter arterial embolization; Therapeutic effect; CT findings; Lecithin

ABBREVIATIONS: Hepatocellular Carcinoma (HCC); Transcatheter Arterial Embolization (TAE); Computed Tomography (CT); Asparate Aminotransferase (AST); Alanine Aminotransferase (ALT); Total Bilirubin (TB); Indrocyanine Green Test (ICGR); Platelet Count (PLt)

INTRODUCTION

The use of transcatheter arterial embolization (TAE) to treat primary hepatocellular carcinoma (HCC) was first reported by Doyon *et al.* in 1974 (1).

There was a point in the 1990s where TAE was not believed to help prolong survival (2-4), but recent prospective randomized studies have indicated its antitumor efficacy as well as its prolongation of life (5-7). TAE is specified as a treatment strategy for HCC in the National Cancer Institute (NCI), Physician Data Query (PDQ), Treatment Option Overview (8), the National Comprehensive Cancer Network (NCCN) Guidelines (9), and the Barcelona Group's treatment algorithm (10). The current research was planned to study the association between pre-treatment abdominal CT findings and the local therapeutic effect of TAE, in order to improve the tumor necrotic action of TAE.

METHODOLOGY

Subjects

The subjects were patients with HCC who underwent treatment along with angiography from March 2000 to April 2003 at Tokyo Women's Medical University Hospital. These patients had no more than 3 tumors that were each superselectively embolized and no tumor staining whatsoever was noted immediately following treatment (indicating complete embolization); in all, 100 nodules in 81 cases were retrospectively studied. The subjects included 60 men and 21 women with a mean age of 68.8 years and their average tumor size was 2.3±1.1cm (**Table 1**).

TABLE 1 Background of Patients

	Mean (SD)
Number of cases	81
Number of nodules	100
Men: women	60:21
Mean age (yo)	68.8 (6.6)
Average tumor size (cm)	2.3 (1.1)
AST (IU/L)	78.0 (66.9)
ALT (IU/L)	64.6 (52.3)
TB (mg/dL)	0.77 (0.47)
ICGR15 (%)	24.7 (11.6)
PLt ($\times 10^4$/mm^3)	12.9 (8.6)

AST: Aspartate aminotransferase; ALT: Alanine aminotransferase; TB: Total bilirubin; ICGR: Indrocyanine green test; PLt: Platelet count

Abdominal-enhanced CT Imaging and Interpretation

Imagining was done at 120kvp, 200mA, and 1.0s using an X Vigor Real from Toshiba Corp., Tokyo. A non-ionic contrast medium, iorersol (Optiray, Tyco Healthcare Japan Ltd., Tokyo) was rapidly infused at 3mL/s: 100-120mL in total) via a peripheral vein. The arterial phase was 30-35s after the start of infusion of contrast medium, and the delayed phase was 1min

Hepato-Gastroenterology 2008; 55:531-534

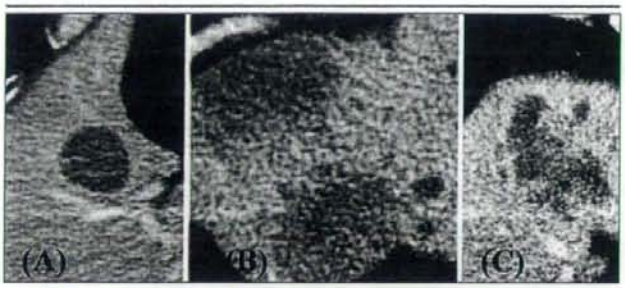

FIGURE 1 Tumors of smooth type **(A)**, irregular type **(B)** and invasive type **(C)**.

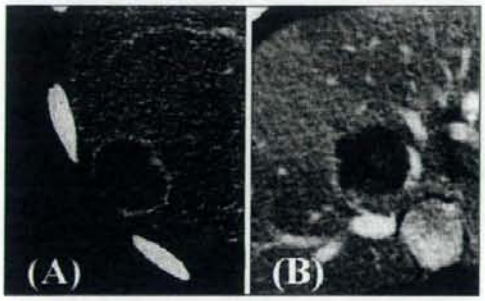

FIGURE 2 Corona-positive tumor **(A)** and corona-negative tumor **(B)**.

50s-2min after the start of infusion of contrast medium, and the entire liver was imaged in a breath-hold for each phase. The speed of the table movement was 7mm/s and the slice thickness was 3-5mm

Interpretation of CT findings was done by a total of 6 individuals: 5 residents at the Institute of Gastroenterology with 6 years of experience and 1 radiology specialist with 8 years or more of experience.

TAE Procedure

Embolization was performed with an iodized oil (Lipiodol Ultra Fluide, Guerbet, France) emulsion with lecithin and gelatin sponge particles. The water phase of the emulsion was 0.086g glycerin to adjust the specific gravity, 0.86mL non-ionic contrast medium, iopamidol (Iopamiron, 61.24%, Nihon Schering K. K., Tokyo), and 20mg doxorubicin hydrochloride: the oil phase was 6.25mg lecithin and 5mL lipiodol, which were mixed at a compounding ratio of 1:4 to prepare the emulsion.

The emulsion was infused until the blood flow to the tumor stopped, after which the tumor was embolized with gelatin sponge particles. The catheters used were a CX Catheter UII (Cathex Co., Ltd., Kanagawa) and a microcatheter (Progreat™, Terumo Corp., Tokyo). The extent of embolization was minimized to the area containing each nodule in accordance with the tumor's location and size. A microcatheter was inserted and the tumor was selectively embolized from some of the segmental branch arteries, subsegmental branch arteries or vessels feeding the tumor.

Assessment of Effects

Tumors with satisfactory accumulation of lipiodol in the tumor on CT findings 1 year after TAE was performed, no enhancement at the treated site in arterial-phase-enhanced CT, and no washout of contrast medium in the parenchymal phase were defined as "completely necrotic nodules".

Pre-TAE Abdominal CT Findings

For the 100 nodules, pre-treatment-enhanced CT findings were classified according to the following 4 (a-d) elements, and the percentage of tumors with no recurrence at the treated site (defined as "complete necrosis") achieved for each finding was examined. Chi-squared test was used for statistical analysis.

Tumor shape (a) is shown in **Figure 1**. Tumors with regular tumor margins in slices, no elevations around the nodule, and no projections or satellite nodules on delayed-phase-enhanced CT were designated "smooth type" (A), while tumors with any of these attributes were designated "irregular type" (B), and those without a nodular shape were designated "invasive type" (C).

The presence of corona (b) is shown in **Figure 2**. Tumors were classified according the presence or absence of a darkly stained portion (corona) appearing in non-cancerous hepatic parenchyma around the tumor on delayed-phase-enhanced CT.

The maximum size of each nodule (c) in horizontal sections of delayed-phase-enhanced CT was measured. For tumors with a corona, the maximum size (diameter) was measured at the inner margin of the corona; for the invasive type, the maximum length was measured.

Tumor location (d) is shown in **Figure 3**. Based

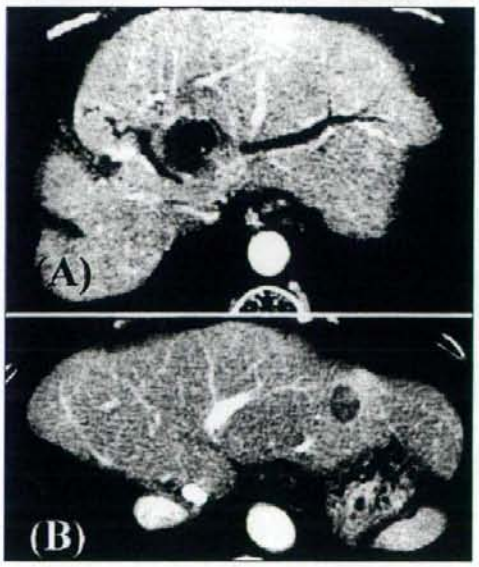

FIGURE 3 Tumors in central location **(A)** and peripheral location **(B)**.

on CT images, the distance from the bifurcation of the left and right branches of the portal vein trunk to the medial margin of the tumor was set as "X", and the distance from the bifurcation of the left and right branches of the portal vein trunk to the liver margin located on an extended line passing through the medial margin of the tumor and the tumor center was set as "L". Nodules with X/L≤1/2 were defined as "in a central location" and those with X/L>1/2 were defined as "in a peripheral location".

RESULTS

The percentage of "complete necrosis" for 100 nodules where TAE was performed was 58% (58/100). The percentage of "complete necrosis" in abdominal-enhanced CT findings was 73.4% (47/64) for smooth type, 34.5% (10/29) for irregular type, and 0.0% (0/7) for invasive type (p=0.0003). The percentage was 67.7% (44/65) for corona-positive tumors and 37.1% (13/35) for corona-negative tumors; corona-positive tumors had a higher frequency of necrosis than corona-negative tumors (p=0.003). In terms of size, tumors with a diameter smaller than 3.0cm had a high frequency of necrosis; in particular, the percentage of "complete necrosis" was 70.0% (28/40) for tumors with a diameter of 1.1-2.0cm and 60.6% (20/33) for tumors with a diameter of 2.1-3.0cm, showing satisfactory results. With regard to tumor location, 64.6% (51/79) of tumors in a peripheral location showed complete necrosis, *vs.* 28.6% (6/21) of those in a central location (p=0.006) **(Table 2)**. p<0.05 was considered to be statistically significant.

TABLE 2 Classification by CT Findings and Response to TAE

Classification	Complete necrosis/ number of treatments	Rate of complete necrosis (%)	p-value
Smooth type	47/64	73.4	0.0003
Irregular type	10/29	34.5	
Invasive type	0/7	0.0	
With corona	44/65	67.7	0.003
Without corona	13/35	37.1	
≤1.0cm	1/2	50.0	
1.1-2.0cm	28/40	70.0	
2.1-3.0cm	20/33	60.6	0.11
3.1-4.0cm	4/13	30.8	
≥4.1cm	2/8	25.0	
Central location	6/21	28.6	0.006
Peripheral location	51/79	64.6	

p<0.05 was considered to be statistically significant.

DISCUSSION

Since many HCCs recur repeatedly, they cannot be successfully treated with single therapy alone, so treatment is wide-ranging. Therefore, studying the effects of one therapy using life expectancy is difficult. Studying antitumor efficacy in treated nodules is believed to be an appropriate method to assess therapy, but there are few detailed studies on the local therapeutic effect of TAE (11). With regard to 71 lesions with no more than 2 concomitant tumors under 5cm, Takayasu *et al.* reported a recurrence rate of 33.2% after 1 year, and that 66.8% had tumor necrosis without local recurrence 1 year after treatment (12). In the current study, 58% had no localized recurrence 1 year after treatment; the characteristics of tumors with a high percentage of "complete necrosis" were "smooth type", "corona-positive", "peripheral location", and tumor size under 3.0cm. There were 33 nodules that satisfied all of these 4 conditions, and of these 33 nodules "complete necrosis" was achieved in 31 cases (93.9%). Based on these results, nodules where a therapeutic effect can be anticipated can be predicted by abdominal enhanced CT findings, and this will prove useful in terms of determining indications for treatment.

The TAE procedure currently in widespread use involves the following: mixing lipiodol with a water-soluble anticancer agent, preparing a water-in-oil emulsion, infusing it into a branch of the arteries feeding the HCC, and later embolizing the same branch with gelatin sponge particles (13-15). As regards water-in-oil emulsions of lipiodol, improvement in the controlled release of anticancer agents and an action to inhibit flow outside the treated tissue have been noted (16-17), and antitumor efficacy and prolongation of life have been reported (18-19). At this hospital, lecithin is added to lipiodol as a surface active agent to produce emulsions with a smaller particle size and better stability. *In vitro*, lipiodol with lecithin is understood to produce an emulsion with a smaller particle size and improve formulation stability (20). Pelletier *et al.* reported that TAE using a lipiodol emulsion with lecithin has substantial antitumor efficacy over TAE with lipiodol emulsions lacking lecithin (4). Methods of minimizing necrosis of non-cancerous areas by superselective TAE immediately in front of the carcinoma using a microcatheter (the same technique as used in the current study) are generally used for embolization (11,12,21). In spite of efforts to improve the therapeutic effect of TAE by devising embolization materials and techniques to completely embolize the blood supply of the cancerous segment containing the HCC nodule, a few cases have been observed where local recurrence soon occurs although TAE is completely performed. One reason for this is that TAE may have been performed even for nodules where a therapeutic effect could not be anticipated. With well-differentiated early HCC, the blood flow from the hepatic artery is minimal and TAE is known to have very little effect (22); for HCC, there may otherwise be conditions that are conducive or nonconducive to TAE. The current results indicated a significant difference in effective tumor necrosis for different tumor shapes, tumors with or without a corona, and different tumor locations.

A corona is a darkly stained portion appearing in non-cancerous hepatic parenchyma around the tumor on portal-venous-phase-enhanced CT, and is a representation of drainage veins for the blood flow inside a tumor (23,24). Thus, a corona may appear if a (plethoric) HCC has blood flow from the hepatic

artery. Corona-positive HCCs are plethoric tumors, so lipiodol readily accumulates and can serve as grounds for anticipating TAE to have an effect, even if arterial phase findings through CT are not confirmed. In addition, a high frequency of necrosis (64%) was achieved for tumors in a peripheral location. At a central location, the inflow of lipiodol is inadequate because feeding arteries bifurcate proximal to the hepatic artery, diminishing the effects of TAE. Based on the above, characteristics for a high likelihood of necrosis in TAE were "smooth type" plus "corona-positive" on portal-venous-phase-enhanced CT with nodules in a peripheral location, and tumor size of no more than 3.0cm. The percentage of "complete necrosis" in HCCs satisfying all these conditions was 93.9%.

If nodules show favorable characteristics in light of the indications, TAE is a treatment that can be anticipated to provide highly effective tumor necrosis, and it can also be performed when other percutaneous therapies are not indicated, such as when there are multiple nodules or the size of the nodule exceeds 3.0cm, showing a wide range of applicability. If proficiency with techniques and the quality of drugs and instruments used in embolization are improved in the future, the efficacy of TAE for tumor necrosis will be further enhanced and this will contribute to prolonging survival in patients with HCC.

REFERENCES

1 **Doyon D, Mouzon A, Jourde AM, Regensberg C, Frileux C:** Hepatic arterial embolization in patients with malignant liver tumours. Ann Radiol 1974; 17:593-603.

2 **No authors listed:** A comparison of lipiodol chemoembolization and conservative treatment for unresectable hepatocellular carcinoma. Groupe d'Etude et de Traitement du Carcinome Hepatocellulaire. N Engl J Med 1995; 332:1256-1261.

3 **Bruix J, Llovet JM, Castells A, Montana X, Bru C, Ayuso MC, et al:** Transarterial embolization *versus* symptomatic treatment in patients with advanced hepatocellular carcinoma: results of a randomized, controlled trial in a single institution. Hepatology 1998; 27:1578-1583.

4 **Pelletier G, Ducreux M, Gay F, Lubonski M, Hagege H, Dao T, et al:** Treatment of unresectable hepatocellular carcinoma with lipiodol chemoembolization: a multicenter randomized trial. Group CHC. J Hepatol 1998; 29:129-134.

5 **Lo CM, Ngan H, Tso WK, Liu CL, Lam CM, Poon RT, et al:** Randomized controlled trial of transarterial lipiodol chemoembolization for unresectable hepatocellular carcinoma. Hepatology 2002; 35:1164-1171.

6 **Llovet JM, Real MI, Montana X, Planas R, Coll S, Aponte J, et al:** Arterial embolization or chemoembolization *versus* symptomatic treatment in patients with unresectable hepatocellular carcinoma: a randomized controlled trial. Lancet 2002; 359:1734-1739.

7 **Llovet JM, Bruix J:** Systematic review of randomized trials for unresectable hepatocellular carcinoma: Chemoembolization improves survival. Hepatology 2003; 37:429-442.

8 NCI-PDQ(http://www.nci.nih.gov) Adult Primary Liver Cancer(PDQ®): Treatment http://www.cancer.gov/cancertopics/pdq/treatment/adult-primary-liver/HealthProfessional/page

9 NCCNClinicalPracticeGuidelineinOncology Http://www.nccn.org/professionals/physician_gls/f_guidelines.asp?button=1+Agree#site

10 **Llovet JM, Burroughs A, Bruix J:** Hepatocellular carcinoma. Lancet 2003; 362:1907-1917.

11 **Matsui O, Kadoya M, Yoshikawa J, Gabata T, Takashima T, Demachi H:** Subsegmental transcatheter arterial embolization for small hepatocellular carcinomas: local therapeutic effect and 5-year survival rate. Cancer Chemother Pharmacol 1994; 33:S84-88. (Suppl)

12 **Takayasu K, Muramatsu Y, Maeda T, Iwata R, Furukawa H, Muramatsu Y, et al:** Targeted transarterial oily chemoembolization for small foci of hepatocellular carcinoma using a unified helical CT and angiography system: analysis of factors affecting local recurrence and survival rates. AJR Am J Roentgenol 2001; 176:681-688.

13 **Nakamura H, Hashimoto T, Oi H, Sawada S:** Transcatheter oily chemoembolization of hepatocellular carcinoma. Radiology 1989; 170:783-786.

14 **Stefanini GF, Amorati P, Biselli M, Mucci F, Celi A, Arieti V, et al:** Efficacy of transarterial targeted treatments on survival of patients with hepatocellular carcinoma. An Italian experience. Cancer 1995; 75:2427-2434.

15 **Rougier P, Roche A, Pelletier G, Ducreux M, Pigno JP, Etienne JP:** Efficacy of chemoembolization for hepatocellular carcinomas: experience from the Gustave Roussy Institute and the Bicetre Hospital. J Surg Oncol Suppl 1993; 3:94-96.

16 **Fukushima S, Juni K, Nakano M:** Preparation of and drug release from w/o/w type double emulsions containing anticancer agent. Chem Pharm Bull 1983; 31:4048-4056.

17 **Takahashi T, Ueda S, Kono K, Majima S:** Attempt at local administration of anticancer agents in the form of fat emulsion. Cancer 1976; 38:1507-1514.

18 **Camma C, Schepis F, Orlando A, Albanese M, Shahied L, Trevisani F, et al:** Transarterial chemoembolization for unresectable hepatocellular carcinoma: meta-analysis of randomized controlled trials. Radiology 2002; 224:47-54.

19 **Nakao N, Uchida H, Kamino K, Nishimura Y, Ohishi H, Takayasu Y, et al:** Determination of the optimum dose level of lipiodol in transcatheter arterial embolization of primary hepatocellular carcinoma based on retrospective multivariate analysis. Cardiovasc Intervent Radiol 1994; 17:76-80.

20 **De Baere T, Zhang X, Aubert B, Harry G, Lagrange C, Ropers J, et al:** Quantification of tumor uptake of iodized oils and emulsions: experimental study. Radiology 1996; 201:731-735.

21 **Matsui O, Kadoya M, Yoshikawa J, Gabata T, Arai K, Demachi H, et al:** Small hepatocellular carcinoma: treatment with subsegmental transcatheter arterial embolization. Radiology 1993; 188:19-20.

22 **Takayasu K, Wakao F, Moriyama N, Muramatsu Y, Sakamoto M, Hirohashi S, et al:** Response of early-stage hepatocellular carcinoma and borderline lesions to therapeutic arterial embolization. AJR Am J Roentgenol 1993; 160:301-306.

23 **Matsui O, Kadoya M, Suzuki M, Inoue K, Itoh H, Ida M, et al:** Work in progress: dynamic sequential computed tomography during arterial portography in the detection of hepatic neoplasms. Radiology 1983; 146:721-727.

24 **Ueda K, Matsui O, Kawamori Y, Nakamura Y, Kadoya M, Yoshikawa J, et al:** Hypervascular hepatocellular carcinoma: evaluation of hemodynamics with dynamic CT during hepatic arteriography. Radiology 2001; 219:298-300.

Identification of Novel Immunohistochemical Tumor Markers for Primary Hepatocellular Carcinoma; Clathrin Heavy Chain and Formiminotransferase Cyclodeaminase

Masanori Seimiya,[1] Takeshi Tomonaga,[1] Kazuyuki Matsushita,[1] Masahiko Sunaga,[1] Masamichi Oh-ishi,[2] Yoshio Kodera,[2] Tadakazu Maeda,[2] Shigetsugu Takano,[3] Akira Togawa,[3] Hideyuki Yoshitomi,[3] Masayuki Otsuka,[3] Masakazu Yamamoto,[4] Masayuki Nakano,[5] Masaru Miyazaki,[3] and Fumio Nomura[1]

Early diagnosis of hepatocellular carcinoma (HCC) greatly improves its prognosis. However, the distinction between benign and malignant tumors is often difficult, and novel immunohistochemical markers are necessary. Using agarose two-dimensional fluorescence difference gel electrophoresis, we analyzed HCC tissues from 10 patients. The fluorescence volumes of 48 spots increased and 79 spots decreased in tumor tissues compared with adjacent nontumor tissue, and 83 proteins were identified by mass spectrometry. Immunoblot confirmed that the expression of clathrin heavy chain (CHC) and Ku86 significantly increased, whereas formiminotransferase cyclodeaminase (FTCD), rhodanese, and vinculin decreased in tumor. The protein expression in tumor and nontumor tissues was further evaluated by immunostaining. Interestingly, CHC and FTCD expression was strikingly different between tumor and nontumor tissues. The sensitivity and specificity of individual markers or a combination for the detection of HCC were 51.8% and 95.6% for CHC, 61.4% and 98.5% for FTCD, and 80.7% and 94.1% for CHC+FTCD, respectively. Strikingly, the sensitivity and specificity increased to 86.7% and 95.6% when glypican-3, another potential biomarker for HCC, was used with FTCD. Moreover, CHC and FTCD were useful to distinguish early HCC from benign tumors such as regenerative nodule or focal nodular hyperplasia, because the sensitivity and specificity of the markers are 41.2% and 77.8% for CHC, 44.4% and 80.0% for FTCD, which is comparable with those of glypican-3 (33.3% and 100%). The sensitivity significantly increased by combination of these markers, 72.2% for CHC+FTCD, and 61.1% for CHC+glypican-3 and FTCD+glypican-3, as 44.4% of glypican-3 negative early HCC were able to be detected by either CHC or FTCD staining. *Conclusion:* Immunostaining of CHC and FTCD could make substantial contributions to the early diagnosis of HCC. (HEPATOLOGY 2008;48:519-530.)

Abbreviations: 2-DE, two dimensional electrophoresis; 2D-DIGE, two dimensional fluorescence difference gel electrophoresis; CHC, clathrin heavy chain; eHCC, early hepatocellular carcinoma; FNH, focal nodular hyperplasia nodules; FTCD, formiminotransferase cyclodeaminase; HCC, primary hepatocellular carcinoma; Ku86, 82-kDa ATP-dependent DNA helicase II; LRN, large regenerative nodule; mRNA, messenger RNA.

From the [1]Department of Molecular Diagnosis, Graduate School of Medicine, Chiba University; [2]Laboratory of Biomolecular Dynamics, Department of Physics, Kitasato University School of Science; [3]Department of General Surgery, Graduate School of Medicine, Chiba University; [4]Department of Surgery, Institute of Gastroenterology, Tokyo Women's Medical University; and the [5]Division of Clinical Investigation, National Hospital Organization, Chiba Medical Center, Chiba, Japan.

Received November 15, 2007; accepted April 1, 2008.

Supported by Grant-in-Aid 18014007, 18659363, 19390330 and 19390154 to T.T. and F.N. from the Ministry of Education, Science, Sports and Culture of Japan and also by the Chiba Serum Institute Memorial Fund for Health Medical Welfare.

Address reprint requests to: Takeshi Tomonaga, Department of Molecular Diagnosis, Graduate School of Medicine, Chiba University, 1-8-1 Inohana, Chuo-ku, Chiba 260-8670, Japan. E-mail: tomonaga@faculty.chiba-u.jp; fax: (81)-43-226-2169.

Published online in Wiley InterScience (www.interscience.wiley.com).

DOI 10.1002/hep.22364

Potential conflict of interest: Nothing to report.

Additional Supporting Information may be found in the online version of this article.

Primary hepatocellular carcinoma (HCC) is a major health problem worldwide.[1,2] It is known that HCC develops from a chronic inflammatory liver disease due to hepatitis B virus and hepatitis C virus infection; therefore, HCC shows especially high prevalence in Asia and Africa, where the rate of hepatitis C virus infection is high.[3] In Japan, HCC has been ranked as the third most common cancer causing death.[4] Screening tests are serological and radiological. Alpha-fetoprotein, lens culinaris agglutinin-reactive fraction of alpha-fetoprotein, and serum protein induced by vitamin K absence or antagonist-II are the most commonly used diagnostic markers for HCC, although their sensitivity and specificity are not high enough and are inadequate for identifying early stage HCC.[5,6] The radiological test most widely used for surveillance is ultrasonography. Although ultrasound is able to detect small nodules of smaller than 2 cm, biopsy of these lesions is recommended for the diagnosis of HCC if the vascular profile on dynamic imaging is not characteristic of HCC.[7] Such small masses range from benign nodules to malignant HCCs, and it is difficult, even for experienced pathologists, to distinguish dysplasia and well-differentiated HCC, especially when the lesion is small; therefore, development of new immunocytochemical markers is needed to diagnose early HCC.

Recently, the human genome project has been completed, and the genome database published. Moreover, high-throughput analysis of proteins has become possible by the development of tandem mass spectrometry technology. The breakthrough of this proteome technology enabled comparative studies of comprehensive protein expression and the identification of protein. As for HCC, proteome analysis using two-dimensional electrophoresis (2-DE), two-dimensional fluorescence difference gel electrophoresis (2D-DIGE), and liquid chromatography have recently been reported.[8-10] Although a number of proteins have been identified as candidate markers for HCC,[11,12] none have been applied in the clinical setting; therefore, a more comprehensive and sophisticated approach is mandatory to find novel proteins associated with HCC. Oh-ishi et al.[13] developed agarose 2-DE, which uses agarose gel in the first dimension. This method not only allows for large-scale quantitative comparisons of protein expression but is also able to resolve high-molecular-mass proteins larger than 150 kDa that are difficult to resolve with immobilized pH gradient (IPGs). We have previously identified several novel proteins with altered expression in primary colorectal cancer and esophageal cancer using agarose 2-DE or agarose 2D-DIGE.[14,15] These techniques appear to have advantages of adequate sensitivity, high reproducibility, and a wide dynamic range.

In this study, we aimed to identify novel biomarkers useful for the diagnosis of HCC. For that purpose, we compared protein expressions between HCC and adjacent nontumor tissues using the agarose 2D-DIGE method. Differentially expressed proteins were validated by immunoblot or immunostaining and were further evaluated for their potential as novel immunohistochemical markers.

Materials and Methods

The following details can be found in the Supplementary Information 1: protein extraction, fluorescent dye (CyDye) labeling, agarose 2D-DIGE, enzymatic in-gel digestion of proteins, identification of proteins, and quantification of messenger RNA (mRNA).

Human Tissue Samples. Ten HCC tissues were obtained at resection in the Department of General Surgery, Chiba University Hospital. The clinical features of these 10 cases are summarized in Table 1. Written informed consent was obtained from each patient before surgery. Excised samples were obtained within 1 hour after the operation from the tumor and adjacent non-tumor tissue. All excised tissues were immediately placed in liquid nitrogen and stored at −80°C until analysis.

Immunoblotting. Protein extracts were separated by electrophoresis on 10% to 20% polyacrylamide gradient gel. Proteins were transferred to polyvinylidene fluoride membranes (Millipore, Bedford, MA) in a tank transfer apparatus (Bio-Rad, Hercules, CA), and the membranes were blocked with 5% skim milk in phosphate-buffered saline. Anti-clathrin heavy chain (CHC) mouse monoclonal antibody (BD Biosciences Pharmingen) diluted 1:4000, anti-82 kDa adenosine triphosphate-dependent DNA helicase II (Ku86) mouse monoclonal antibody (COSMO BIO Co., Ltd, Tokyo, Japan) diluted 1:4000, anti-vinculin mouse monoclonal antibody (Upstate Biotechnologies, NY) diluted 1:8000, anti-formiminotransferase cyclodeaminase (FTCD) rabbit polyclonal

Table 1. Clinical Features of Patients with HCC

No.	Age	Sex	Virus	Size (mm)	Adjacent Tissue	AJCC Stage
1	69	Male	–	70 × 70	Normal	III
2	65	Male	HCV	60 × 45	LC	III
3	76	Male	–	55 × 45	CH	III
4	80	Male	HCV	30 × 38	LC	II
5	58	Female	–	45 × 40	LC	II
6	61	Male	HCV	35 × 32	CH	II
7	65	Male	HCV	25 × 16	LC	II
8	75	Male	HCV	25 × 23	CH	I
9	75	Male	HCV	25 × 20	LC	II
10	79	Male	HCV	110 × 90	CH	III

HCV, hepatitis C virus; LC, liver cirrhosis; CH, chronic hepatitis.

antibody (Abcam, Cambridge, UK) diluted 1:2000, and anti-thiosulfate sulfurtransferase (rhodanese) rabbit polyclonal antibody (Santa Cruz Biotechnology Inc., Santa Cruz, CA) diluted 1:1000 in blocking buffer were used as primary antibodies. Goat anti-mouse immunoglobulin G (IgG) horseradish peroxidase (Bio-Rad Laboratories, Hercules, CA) diluted 1:3000, and rabbit antigoat IgG horseradish peroxidase (Cappel, West Chester, PA) diluted 1:500 in blocking buffer were used as secondary antibodies. Antigens on the membrane were detected with enhanced chemiluminescence detection reagents (GE Healthcare).

Immunohistochemistry. From 20 HCC specimens (five well-differentiated, 10 moderately differentiated, and five poorly differentiated HCC), paraffin-embedded blocks of tumor and adjacent nontumor tissue were collected in the Department of General Surgery, Chiba University Hospital. Four-μm sections from paraffin tissue were fixed on slide glasses. In addition, tissue arrays (CA3, CSN3, CS3; SuperBio-Chips, Seoul, Korea) were used for immunohistochemistry, which contained 83 tumor (14 well differentiated, 40 moderately differentiated, 11 poorly differentiated, and 18 unclassified HCC) and 68 nontumor liver tissues. Two adenoma specimens were obtained from the Division of Clinical Investigation, National Hospital Organization, Chiba Medical Center. Three large regenerative nodules (LRN), five focal nodular hyperplasia nodules (FNH), and 18 early HCC (eHCC) specimens were obtained from the Institute of Gastroenterology, Tokyo Women's Medical University Hospital. Tissues were deparaffinized in xylene and rehydrated by reducing the concentration of ethanol (100%, 100%, and 70%, 5 minutes each). Antigents were unmasked with microwave irradiation for 5 minutes in pH 6.0 citric buffer three times. Primary antibodies were diluted as follows. Anti-CHC antibody diluted 1:200, anti-FTCD antibody diluted 1:200, anti-rhodanese antibody diluted 1:100, and anti-Glypican-3 antibody (Biomosaics, Burlington, VT) diluted 1:100 in blocking buffer. EnVision + system (DAKO Japan, Kyoto, Japan) was used to visualize tissue antigens. Tissue sections were counterstained with hematoxylin for 1 minute. Protein expression was scored as negative (0), weak (1), moderate (2), and strong (3). Two pathologists evaluated immunohistochemical staining of the samples. The results of the evaluation agreed in 96.0% of cases. When the results were discordant, the judgment was made by the other investigator.

Results

Identification of Altered Expressed Proteins in Human HCC Tissue. To search for novel biomarkers useful for the diagnosis of HCC, we used the agarose 2D-DIGE method to explore proteins differently expressed between HCC and adjacent nontumor tissues. Each nontumor sample was labeled with Cy3, each cancer sample was labeled with Cy5, and pooling aliquots were labeled with Cy2, respectively. These labeled proteins were mixed and separated in the same 2D gel (Fig. 1A). Protein spots that were increased or decreased in tumor tissues were displayed as red or green, respectively. These spots were detected and quantitated with DeCyder imaging analysis software, and then statistical analysis was performed across the 10 gels. The fluorescence volumes of 48 spots increased and 79 spots decreased in cancer tissues compared with adjacent nontumor tissue (Student t test, $P < 0.05$). To identify the proteins, 500 μg whole-cell lysates of HCC or nontumor tissues (Table 1; cases 1 and 2) were separated by conventional agarose 2-DE, and proteins were visualized by Coomassie blue staining (Fig. 1B). We carefully compared the DIGE image with Coomassie blue staining gels and picked altered protein spots manually. A total of 101 (83 proteins) of 127 spots were identified by mass spectrometry (Tables 2 and 3). The expression of these identified proteins was differentially expressed in most of the 2D-DIGE gel (Tables 2 and 3). Although many have previously been reported as differentially expressed proteins in HCC, which we were able to reproduce using a proteomic approach, a few were further tested for their clinical use. Moreover, most down-regulated proteins were related to detoxification and metabolism, which probably reflect liver dysfunction accompanying the development of HCC. Thus, we made an attempt to find proteins that could be potential diagnostic markers for HCC.

Validation of Differentially Expressed Protein Between Tumor and Nontumor Tissues. Although 2-DE is a powerful technique, multiple proteins may be included in one spot, leading to misinterpretation of the results. Therefore, to confirm the difference of protein expression between tumor and nontumor tissues, validation using other methods is essential. Thus, immunoblot analyses of several proteins with commercially available antibodies were performed to confirm the differential protein expression in tumor tissues. CHC and Ku86 were up-regulated, whereas FTCD, rhodanese, and vinculin were down-regulated in most tumor tissues (Fig. 2). It is interesting to note that a ladder of smaller bands below full-length vinculin was observed and one of the bands around 60 kDa, which might be cleaved products of vinculin, was stronger in nontumor tissues than in tumor tissues.

Quantification of mRNA Levels. Differentially expressed proteins are commonly regulated at the transcrip-

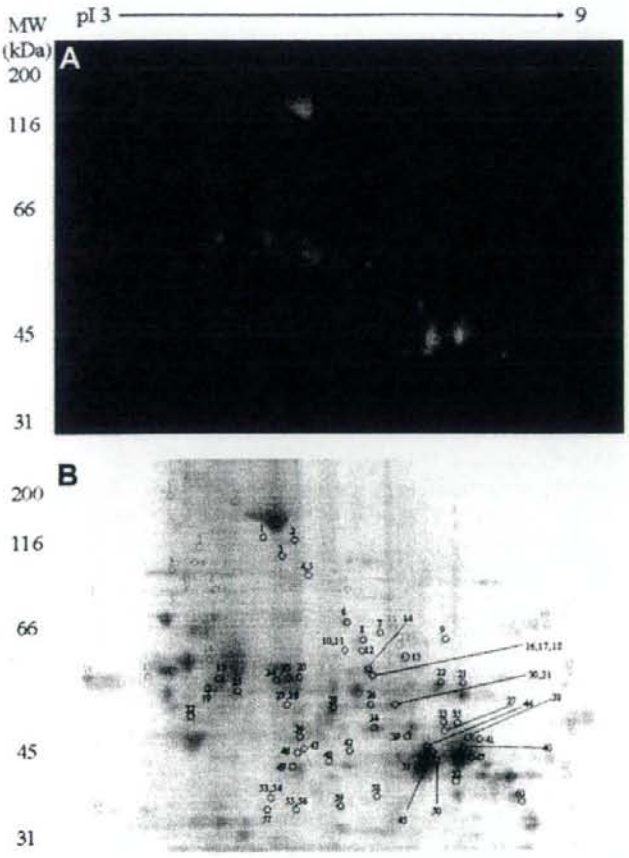

Fig. 1. Proteome analysis of HCC tissues using agarose 2D-DIGE and agarose 2-DE. Whole-cell lysates were prepared from matched samples of tumor tissue, adjacent nontumor tissue, and pooling aliquots (internal control). (A) Increased protein spots in tumor tissues are displayed in red (Cy5), and decreased protein spots in tumor tissues are displayed in green (Cy3). (B) Conventional agarose 2-DE patterns were visualized by Coomassie Blue staining. Protein spots cut from this gel were identified by mass spectrometry and are shown in red circles (up-regulated in HCC) or black circles (down-regulated in HCC). 2D-DIGE, two-dimensional fluorescence difference gel electrophoresis.

tional level or through translational and posttranslational modifications. To explore the mechanisms leading to the changes of protein expression, we examined the mRNA level of the proteins by quantitative reverse transcription polymerase chain reaction. The mRNA levels of FTCD, rhodanese, and vinculin were decreased in most tumor tissues, consistent with the changes of protein expression. In contrast, CHC and Ku86 mRNA levels did not correlate with their protein expression levels (Fig. 3); therefore, overexpression of CHC and Ku86 in tumor tissues does not occur at the transcriptional level.

Immunohistochemical Analysis. Although there was no bias in the cellularity of tumor and adjacent nontumor tissues, whole tissue sections included nonhepatic parenchymal cells, and the altered protein expression in our 2-DE analysis may emanate from such nonhepatocyte components. Thus, the differential protein expression in HCC was also validated by immunohistochemistry to examine the localization of identified proteins. Paraffin-embedded tumor tissue and adjacent nontumor tissues of all 20 cases were stained with antibodies that were used in immunoblot analysis (Fig. 4). CHC has been reported to localize in the plasma membrane and the cytoplasmic face of intracellular organelles. Although no staining of CHC was observed in nontumor tissues, tumor cells showed scattered staining in the cytoplasm and plasma membrane (Fig. 4A). Bile duct, endothelial cell, and Kupffer cells were also positively stained. FTCD showed strong and uniform staining in the cytoplasm of nontumor tissue compared with faint staining in the cytoplasm of tumor cells (Fig. 4B). Rhodanese showed a mixture of scattered and strong staining in the cytoplasm of nontumor tissue, whereas tumor tissue was scarcely stained (Fig. 4C). These results confirmed the differential expression of proteins between tumor and nontumor tissues.

Clinical Application. Discrimination of well-differentiated HCC and nontumor tissues within a cirrhotic liver is often difficult even for experienced pathologists, and additional immunohistochemical markers are

Table 2. Protein Expression in HCC and Adjacent Nontumorous Tissue

Protein Increased in Tumor Tissue									
No	Database Accession No.	Protein Name	Average Mass	Homogeneity Rate (%)	T-test	Score	Coverage (%)	Fold Increase	References*
T1	gi-2506872	Fibronectin precursor	262,586	80	0.035	73.8	3.2	1.53	(1)†
T2	gi-4758012	Clathrin heavy chain 1	191,595	89	<0.001	42.2	3.1	2.26	
T3	gi-19913410	Major vault protein	99,248	100	<0.001	82.4	8.6	1.73	(2)
T4	gi-2804273	Alpha actinin 4	102,250	78	0.008	88.6	10.3	1.36	
T5	gi-4507677	Tumor rejection antigen (gp96)	92,450	90	0.022	167.4	20.2	1.67	(3)†
T6	gi-6005942	Valosin-containing protein	89,247	90	0.028	128.2	18.4	1.49	(4)
T7	gi-34304590	Heat shock 90kDa protein 1 beta	83,194	100	0.002	51.9	7.0	2.13	(5)†
T8	gi-10863945	82-kDa ATP-dependent DNA helicase II (Ku86)	82,686	100	0.020	53.0	8.0	3.04	
T9	gi-4506077	Protein kinase C substrate 80K-H isoform 1	59,278	78	<0.001	52.5	10.7	1.69	
T10	gi-862457	Enoyl-CoA hydratase	82,888	80	0.021	43.0	6.8	2.09	(6)‡
T11	gi-4557385	Complement component 3 precursor	187,027	80	0.014	88.1	5.3	1.71	(7)
T12	gi-4389275	Albumin complex with myristic/tri-liodobenzoicacid	66,017	100	0.001	127.0	17.1	1.43	
T13	gi-37267	Transketolase	67,732	88	0.036	70.0	9.7	2.67	(8)†
T14	gi-129379	60kDa Heat shock protein, mitochondrial precursor	60,998	83	0.004	139.4	21.2	1.88	(5)†
T15	gi-576554	Antithrombin III variant	52,673	75	0.041	30.4	8.4	1.53	(9)†
T16	gi-4757900	Calreticulin precursor	48,123	100	0.017	83.3	15.4	1.52	(10)†
T17	gi-2506774	Keratin, type II cytoskeletal 8 (Cytokeratin 8)	53,623	88	0.008	150.2	32.5	2.29	
T18	gi-4504505	Hydroxysteroid (17-beta) dehydrogenase 4	79,668	100	0.015	57.2	8.3	2.09	(11)†
T19	gi-24497583	Aldo-ketoreductase family 1, member C3	36,835	90	0.038	114.3	25.7	1.86	(12)
T20	gi-4504447	Heterogeneous nuclear ribonucleoprotein A2/B1 isoform A2	35,987	88	0.008	40.6	12.3	1.44	
T21	gi-21735621	Mitochondrial malate dehydrogenase precursor	35,485	88	0.037	53.3	18.7	1.28	(13)
T22	gi-5031765	11-Beta-hydroxysteroid dehydrogenase 1	32,382	88	0.037	21.3	4.2	1.28	
T23	gi-30584583	Homo sapiens tyrosine 3-monooxygenase	29,250	90	<0.001	93.5	37.2	2.16	

*The references details can be found in Supplementary Information 2.

†Previously reported to be up-regulated in HCC.

‡Previously reported to be down-regulated in HCC.

needed. Although the expression level of CHC and FTCD was strikingly different between tumor and nontumor tissues, analysis of 10 cases is not enough to consider CHC and FTCD as potential histological markers for HCC. Also the histology of nontumor tissues of the 10 cases was variable. To validate the usefulness of CHC and FTCD staining for the diagnosis of HCC, we obtained a commercial tissue array of HCC in which the degree of tumor differentiation and clinicopathological features had been proven (Table 4). The expression level of CHC and FTCD was scored as 0, 1, 2, or 3 by the staining intensity of the proteins. Most HCC tissues showed strong CHC expression (score 3) and negative to weak (score 0, 1) FTCD expression (43 of 83 cases and 51 of 83 cases). In contrast, most non-HCC tissues showed negative to moderate CHC expression (score 0, 1, 2) and moderate to strong FTCD (score 2, 3) expression (65 of 68 cases and 67 of 68 cases) (Table 5A). The sensitivity and specificity for the diagnosis of HCC using CHC expression level above were 51.8% and 95.6%, whereas those using FTCD expression level were 61.4% and 98.5%, respectively. If the combination of CHC and FTCD expression levels were used, the sensitivity and specificity for the diagnosis of HCC were 80.7% and 94.1%, respectively (Table 5B). Interestingly, CHC and FTCD expression level in tumor tissues correlates with tumor differentiation (well-differentiated HCC, 21.4%, 28.6%; moderately differentiated HCC, 52.5%, 15.0%; poorly differentiated HCC, 72.7%, 9.1%, respectively) (Table 5C). CHC and FTCD expression levels did not correlate with other clinicopathological features (age, sex, stage, and tumor size) (data not shown). These results indicated that immunostaining of CHC and FTCD could contribute to the pathological diagnosis of HCC.

Glypican-3 has been reported as a promising marker in the distinction between HCC and nonmalignant hepatocellular lesions.[16,17] Therefore, we compared the diagnostic value of CHC and FTCD for HCC with that of glypican-3 and also examined whether the combination of the three potential markers can improve the diagnostic accuracy of HCC. The sensitivity and specificity of glypican-3 were 62.7% and 97.1%, respectively, which were comparable with those of CHC or FTCD (Table 5B). Strikingly, the sensitivity and specificity increased to

Table 3. Protein Expression in HCC and Adjacent Nontumorous Tissue

No	Database Accession No.	Protein Name	Average Mass	Homogeneity Rate (%)	T-test	Score	Coverage (%)	Fold Decrease	References*
N1	gi-24657579	VCL protein (VINCULIN)	116,718	100	0.015	58.3	6.0	1.81	
N2	gi-1709947	Pyruvate carboxylase, mitochondrial precursor	129,533	70	0.007	137.3	10.8	1.70	(14)†
N3	gi-4938304	Lysine-ketoglutarate reductase	102,064	90	<0.001	62.8	6.9	1.55	
N4	gi-19353009	Similar to elongation factor 2b	57,455	100	0.008	30.8	6.2	1.39	
N5	gi-8659555	Aconitase 1	98,318	100	0.008	151.5	18.8	1.39	
N6	gi-31415705	Transferrin	76,981	75	0.006	128.0	17.4	1.60	
N7	gi-40789249	Aspartyl-tRNA synthetase 2 (mitochondrial)	73,498	100	0.011	36.0	9.0	2.13	
N8	gi-12655193	Phosphoenolpyruvate carboxykinase 2 (mitochondrial)	70,635	75	0.025	189.4	20.1	1.86	
N9	gi-11761629	Fibrinogen, alpha chain isoform alpha preproprotein	69,695	80	0.003	86.9	17.9	2.07	
N10	gi-284351	Phosphoglucomutase	61,352	89	0.004	38.8	6.0	1.48	
N11	gi-4758312	Electron-transferring-flavoprotein dehydrogenase	68,489	89	0.004	82.6	12.3	1.48	
N12	gi-4557645	Heterogeneous nuclear ribonucleoprotein L isoform a	60,169	100	0.007	41.7	10.4	1.74	
N13	gi-20149621	Hypothetical protein LOC26007	58,892	100	0.001	168.6	35.1	2.29	
N14	gi-4557014	Catalase	59,700	89	0.010	161.6	15.4	1.62	(15)†
N15	gi-11140815	Formiminotransferase cyclodeaminase	58,871	100	0.004	158.6	20.3	2.26	
N16	gi-7431380	Uridine diphosphoglucose dehydrogenase	55,040	100	0.032	31.0	7.7	1.31	
N17	gi-4507813	UDP-glucose dehydrogenase	54,971	100	0.032	50.0	12.4	1.31	
N18	gi-4503375	Dihydropyrimidinase	56,575	100	0.032	60.7	8.7	1.31	
N19	gi-25108887	Aldehyde dehydrogenase family 7 member A1	55,348	78	0.003	25.2	6.0	1.71	
N20	gi-4885281	Glutamate dehydrogenase 1	61,379	100	<0.001	181.0	26.8	1.42	
N21	gi-13027638	UDP-glucose pyrophosphorylase 2 isoform a	56,947	100	<0.001	119.6	23.4	2.37	
N22	gi-7705688	Leucine aminopeptidase	56,031	100	<0.001	94.0	17.4	2.44	
N23	gi-28949044	Human mitochondrial aldehyde dehydrogenase	54,426	100	0.023	101.3	15.2	1.49	(16)
N24	gi-20151189	Human glutamate dehydrogenase-apo form	55,990	100	<0.001	181.0	26.8	1.74	
N25	gi-16306550	Selenium binding protein 1	52,339	100	0.010	90.0	18.8	1.42	
N26	gi-22547189	Serine hydroxymethyl transferase 1 (soluble) isoform 2	48,978	89	0.010	89.7	22.1	2.30	
N27	gi-4503481	Eukaryotic translation elongation factor 1 gamma	50,100	100	0.001	30.9	5.8	2.23	
N28	gi-6730018	Human L-arginine:glycine amidinotransferase	44,625	100	0.001	163.7	26.5	2.23	
N29	gi-5031751	3-Hydroxy-3-methylglutaryl-coenzyme A synthase 2	56,581	80	0.007	170.1	22.1	1.66	
N30	gi-19743875	Fumarate hydratase precursor	54,619	89	<0.001	121.0	27.2	2.31	
N31	gi-16878083	Enolase 3	46,884	89	<0.001	49.3	12.4	2.31	
N32	gi-4557888	Keratin 18	48,010	86	0.037	134.9	18.2	1.41	(17)
N33	gi-16950633	Argininosuccinate synthetase	46,482	100	<0.001	84.4	16.9	3.58	(18)†
N34	gi-4530461	Betaine-homocysteine methyltransferase	44,980	100	<0.001	139.0	33.4	5.19	
N35	gi-28178832	Isocitrate dehydrogenase 2 (NADP+), mitochondrial	50,891	90	0.001	110.0	27.0	2.09	
N36	gi-4557587	Fumaryl acetoacetate hydrolase (fumary lacetoacetase)	46,326	100	0.001	106.5	24.1	2.17	(19)
N37	gi-7110715	SEC14-like 2	46,127	89	0.038	83.3	17.6	1.69	
N38	gi-12804931	Acetyl-coenzyme A acyltransferase 2	41,906	100	0.001	119.4	29.4	2.27	
N39	gi-7542837	Medium-chain acyl-CoA dehydrogenase	46,570	88	<0.001	88.6	18.4	1.71	
N40	gi-4557237	Acetyl-coenzyme A acetyltransferase 1 precursor	45,181	78	<0.001	138.4	35.3	1.90	
N41	gi-4501853	Acetyl-coenzyme A acyltransferase 1	44,273	71	0.046	56.7	9.3	1.68	
N42	gi-4504067	Aspartate aminotransferase 1	46,229	100	0.018	95.7	21.7	2.00	
N43	gi-3337390	Haptoglobin	38,215	100	0.001	34.5	8.0	1.74	(20)
N44	gi-4501929	Class I alcohol dehydrogenase, alpha subunit	39,840	88	<0.001	121.2	23.0	4.12	
N45	gi-494091	Chain A, alcohol dehydrogenase (beta-1 isoenzyme)	39,606	100	0.019	84.8	20.4	3.67	
N46	gi-20530221	BLOCK 25	37,747	80	0.029	30.0	18.8	2.34	
N47	gi-13096743	Chain A, human gamma-2 alcohol dehydrogenase	39,676	100	<0.001	106.6	20.9	4.21	
N48	gi-25777615	Proteasome 26S non-ATPase subunit 7	37,007	80	0.006	21.4	7.3	1.86	(21)
N49	gi-1352403	Fructose-1,6-bisphosphatase 1	36,810	100	<0.001	150.4	43.9	2.28	
N50	gi-4507155	Sorbitol dehydrogenase	38,293	90	0.005	69.2	21.9	2.06	
N51	gi-113611	Fructose-bisphosphate aldolase B (liver-type aldolase)	39,455	100	0.003	137.9	28.2	2.59	
N52	gi-1705823	Aldo-ketoreductase family 1 member C4	37,097	100	0.045	110.0	26.6	1.38	(21)
N53	gi-688031	Aryl sulfotransferase ST1A3	34,191	89	0.003	30.4	11.8	2.63	
N54	gi-8815565	Alcohol/hydroxysteroid sulfotransferase	33,747	89	0.003	29.3	8.6	2.63	
N55	gi-9506741	Glycine N-methyltransferase	32,724	75	0.004	42.4	13.6	2.28	
N56	gi-12654663	Esterase D/formylglutathione hydrolase	31,502	75	0.004	56.5	22.1	2.28	
N57	gi-9087220	Sulfotransferase 1A1 (arylsulfotransferase 1)	34,179	100	0.009	84.0	28.6	2.01	
N58	gi-17402865	Thiosulfate sulfurtransferase (rhodanese)	33,410	100	<0.001	99.5	28.2	1.58	
N59	gi-4503607	Electron transfer flavoprotein, alpha polypeptide	35,061	90	<0.001	120.8	43.9	1.72	
N60	gi-4503301	2,4-Dienoyl CoA reductase 1 precursor	36,049	89	0.004	91.5	24.2	1.76	

*The references can be found in Supplementary Information 2.

†Previously reported to be down-regulated in HCC.

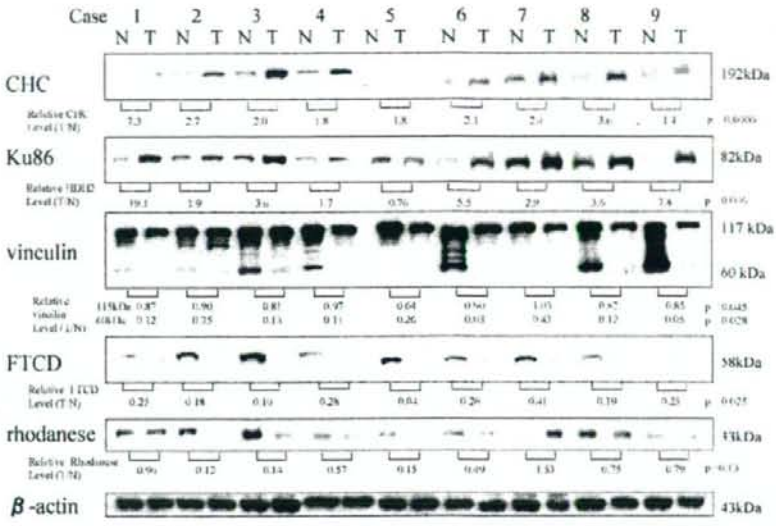

Fig. 2. Immunoblot analysis of differential protein expression in tumor tissues. Total protein lysates prepared from nine matched samples of tumor (T) and adjacent nontumor tissue (N) were separated by electrophoresis on 10% to 20% polyacrylamide gradient gel, and immunoblotted with anti-clathrin heavy chain (CHC) antibody, anti-82 kDa adenosine triphosphate-dependent DNA helicase II (Ku86) antibody, anti-vinculin antibody, anti-formiminotransferase cyclodeaminase (FTCD) antibody, anti-rhodanese antibody, and anti-β-actin antibody (loading control). The intensity of each band was measured with NIH Image, and these proteins levels between tumor and nontumor tissue, normalized with β-actin, were calculated. The expressions of CHC and Ku86 were increased in tumor tissues, whereas vinculin, FTCD, and rhodanese were decreased in tumor tissues.

86.7% and 95.6% when glypican-3 was used with FTCD. These results indicate that combination of the three markers greatly improves the diagnostic accuracy of HCC.

It has recently been recommended to perform a biopsy to identify the features of malignancy when small hepatic masses are detected. As a result, a distinction among regenerative, dysplastic, and malignant hepatocellular nodules is needed on liver biopsy specimens. Therefore, we tested whether we can distinguish eHCC from benign tumors such as dysplastic and regenerative nodules. A total of 18 eHCC tissues and 10 benign tumor tissues (five FNH, three LRN, and two adenomas) were immunostained with CHC, FTCD, and glypican-3 antibodies (Table 6). Note that high-grade dysplastic nodules were included in eHCC because they have been considered as premalignant or malignant lesions by abnormally increased arteriolar and capillary supply.[18] In contrast, low-grade dysplastic nodules were included in benign tumor. Seven eHCCs were distinguished from adjacent nontumor tissues by stronger staining of CHC, whereas one of FNH and LRN was weakly stained with CHC antibody (Fig. 5A, Table 6). Eight eHCCs showed weaker staining of FTCD than adjacent nontumor tissues (Fig. 5B, Table 6). In contrast, all of the FNH and LRN tissues were moderately stained, which is indistinguishable from their adjacent nontumor tissues. Two adenoma tissues showed weaker staining of FTCD than nontumor tissues. Six eHCCs and none of the benign tumors showed stron-

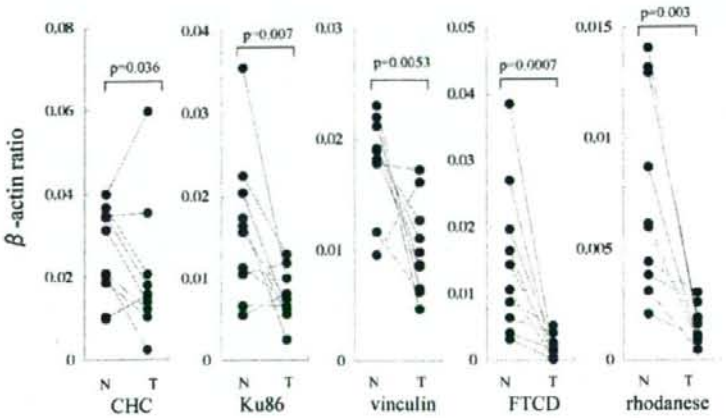

Fig. 3. Quantification of mRNA levels in tumor tissues. Total RNAs were prepared from nine matched samples of tumor (T) and adjacent nontumor tissue (N), and real-time quantitative reverse transcription polymerase chain reaction of CHC (clathrin heavy chain), Ku86 (anti-82-kDa ATP-dependent DNA helicase II), vinculin, FTCD (formiminotransferase cyclodeaminase), and rhodanese mRNA was performed using a LightCycler. These mRNA levels were normalized by β-actin level.

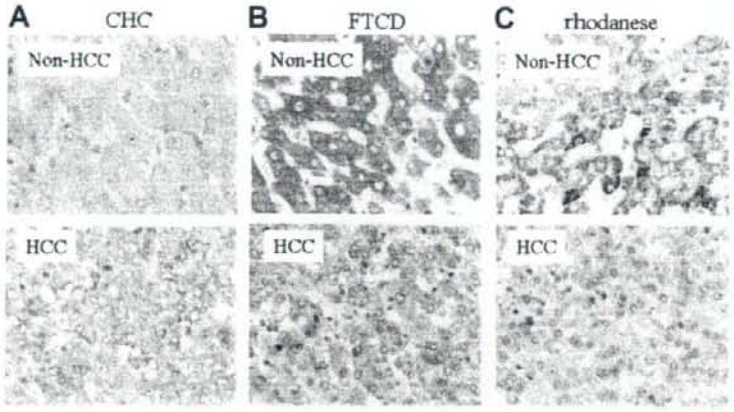

Fig. 4. Immunohistochemical analyses of differential protein expression in tumor tissues. From HCC specimens, paraffin-embedded blocks of tumor and adjacent nontumor tissue were collected. Four-micron sections from paraffin tissue were fixed on slide glasses. The primary antibody is equal to immunoblot analysis. EnVision + system was used to visualize tissue antigens, and tissue sections were counterstained with hematoxylin. (A) Although no staining of CHC (clathrin heavy chain) was observed in nontumor tissues, tumor cells showed scattered staining in the cytoplasm and plasma membrane. (B) FTCD (formiminotransferase cyclodeaminase) showed strong and uniform staining in the cytoplasm of nontumor tissue compared with faint staining in the cytoplasm of tumor cells. (C) Rhodanese showed a mixture of scattered and strong staining in the cytoplasm of nontumor tissue, whereas tumor tissue was scarcely stained.

ger staining of glypican-3 than adjacent nontumor tissues. The sensitivity and specificity of CHC, FTCD, and glypican-3 individually for detection of early HCC was 41.2% and 77.8% for CHC, 44.4% and 80.0% for FTCD, and 33.3% and 100% for glypican-3 (Table 6). The sensitivity of CHC or FTCD was better than that of glypican-3. Moreover, the sensitivity significantly increased by combination of these markers, 72.2% for CHC + FTCD, 61.1% for CHC + glypican-3 and FTCD + glypican-3. This is because 44% of glypican-3–negative eHCCs were able to be detected by either CHC or FTCD staining. These results support that CHC and FTCD are potential biomarkers for early detection of HCC.

Table 4. Histology of HCC and Non-HCC Tissues on Tissue Array

	Histology	Case
HCC tissue	Well-differentiated HCC	14
	Moderately differentiated HCC	40
	Poorly differentiated HCC	11
	Unclassified	18
Non-HCC tissue	Chronic hepatitis	8
	Cirrhosis	19
	Dysplastic nodule	1
	Nonspecific reactive change	11
	Reactive hepatitis	20
	Unknown	9

Discussion

In this study, we compared protein expressions between HCC and adjacent nontumor tissues using a proteome method. A total of 83 proteins with altered expression were identified. Validation of the differentially expressed protein by immunoblot or immunostaining demonstrates that CHC, Ku86, FTCD, rhodanese, and vinculin showed striking differences between tumor and nontumor tissues. Evaluation of the staining intensity of CHC and FTCD enabled us not only to distinguish nontumor and tumor tissues with high accuracy but to discriminate eHCC and benign tumors such as dysplastic and regenerative nodules, which is challenging for expert pathologists. Moreover, CHC and FTCD were able to detect several glypican-3–negative eHCCs, which considerably improved the diagnostic accuracy of eHCC by combination of these markers.

In recent years, the incidence of HCC has been increasing in a number of countries, including Europe and the United States.[19] As a result, considerable emphasis is now placed on the surveillance of HCC. Recent guidelines for HCC management recommend the combined use of alpha-fetoprotein and ultrasonography for HCC surveillance.[7] When small hepatic masses of 1 to 2 cm within a cirrhotic liver are detected, these lesions should undergo biopsy if they do not exhibit typical radiological features of HCC. Accordingly, a distinction between benign and malignant tumor is demanded for pathologists in small

Table 5. Immunohistochemical Analysis From Tissue Array of HCC

A

	CHC		FTCD		Glypican-3	
Expression	Non-HCC	HCC	Non-HCC	HCC	Non-HCC	HCC
3	3	43	45	12	0	38
2	27	33	22	20	2	14
1	31	6	1	32	49	13
0	7	1	0	19	17	18

B

	HCC (n = 83)		Non-HCC (n = 68)		Sensitivity (%)	Specificity (%)
	+	−	+	−		
CHC = 3	43	40	3	65	51.8	95.6
FTCD ≤ 1	51	32	1	67	61.4	98.5
Glypican-3 ≥ 2	52	31	2	66	62.7	97.1
CHC = 3 or FTCD ≤ 1	67	16	4	64	80.7	94.1
CHC = 3 or Glypican-3 ≥ 2	59	24	6	62	71.1	91.2
FTCD ≤ 1 or Glypican-3 ≥ 2	72	11	3	65	86.7	95.6

C

	CHC				FTCD			
Expression	Non-HCC	Well	Moderate	Poor	Non-HCC	Well	Moderate	Poor
3	3 (4.4%)	3 (21.4%)	21 (52.5%)	8 (72.7%)	45 (66.2%)	4 (28.6%)	6 (15.0%)	1 (9.1%)
2	27 (39.7%)	6 (42.9%)	18 (45.0%)	3 (27.3%)	22 (32.4%)	4 (28.6%)	9 (22.5%)	4 (36.4%)
1	31 (45.6%)	4 (28.6%)	1 (2.5%)	0 (0%)	1 (1.5%)	4 (28.6%)	16 (40.0%)	4 (36.4%)
0	7 (10.3%)	1 (7.1%)	0 (0%)	0 (0%)	0 (0%)	2 (14.3%)	9 (22.5%)	2 (18.2%)

biopsies, and further immunohistochemical markers with sufficient sensitivity and specificity are desired. Some markers that can distinguish HCC from dysplastic nodules in cirrhosis have recently been reported.[17] The diagnostic yield of three putative HCC markers, HSP70, glypican 3, glutamine synthetase, was investigated; these were previously proposed by other researchers as promising markers for HCC. However, we identified two novel proteins, CHC and FTCD, by comprehensive proteome analysis, and they were found to be useful for the pathological diagnosis of HCC. Diagnostic values, such as the sensitivity and specificity of proteins for HCC, are comparable to glypican-3 in our analyses. More importantly, the sensitivity and specificity significantly increased when immunostaining of glypican-3 was used with that of CHC and FTCD. Thus, a combination of these markers is useful for screening of HCC.

Table 6. Immunohistochemical Analysis of CHC, FTCD, and Glypican 3 in Early HCC Tissues

	Early HCC		Benign Tumor			
	T > N or T < N	T = N	T > N or T < N	T = N	Sensitivity (%)	Specificity (%)
CHC	7	10	2	7	41.2	77.8
FTCD	8	10	2	8	44.4	80.0
Glypican-3	6	12	0	10	33.3	100

T, tumor tissues; N, nontumor tissues.

Overexpression of CHC in HCC was confirmed by immunoblotting, and most HCC showed strong and scattered staining in the cytoplasm and plasma membranes. Although CHC overexpression has not been reported in any other primary human cancers, fusion of the CHC gene to other genes, such as ALK and TFE3, has been documented in large B-cell lymphoma, pediatric renal adenocarcinoma, and inflammatory myofibroblastic tumor.[20-24] These results indicate that deregulated expression of CHC might play important roles for tumorigenesis. CHC is known to be localized in the plasma membrane and the cytoplasmic face of intracellular organelles in the plasma membrane, called coated vesicles and coated pits. These specialized organelles are involved in the intracellular trafficking of receptors and endocytosis of a variety of macromolecules.[25] Recently, Royle et al.[26] showed that clathrin stabilizes fibers of the mitotic spindle to aid the congression of chromosomes. Because deregulation of mitotic processes leads to chromosomal instability, known as marker of cancer, the importance of clathrin in normal mitosis may be relevant to understanding human cancers. We have previously shown that kinetochore proteins, CENP-A and CENP-H, are upregulated in human primary colon cancer, and their

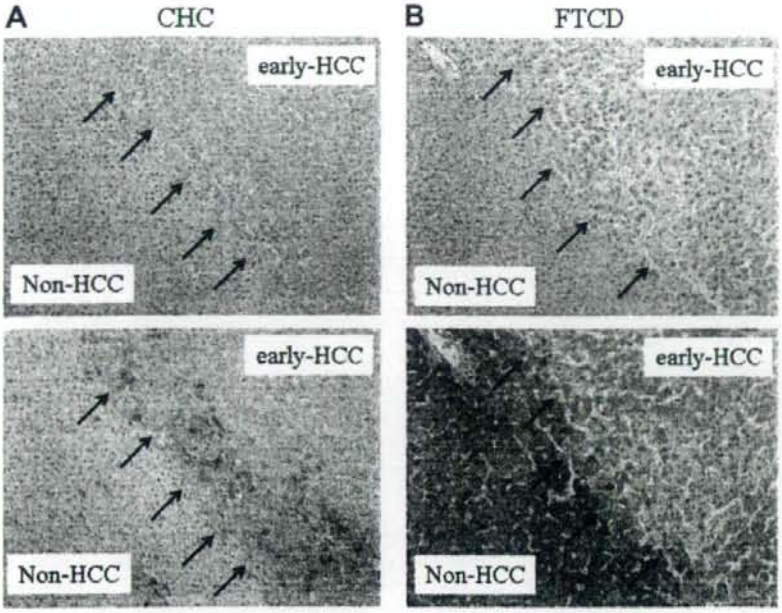

Fig. 5. Immunohistochemical analyses of differential protein expression in early HCC tissues. Early HCC tissues were stained with hematoxylin-eosin (upper panel) or with anti-CHC (clathrin heavy chain)/FTCD (formiminotransferase cyclodeaminase) antibody (lower panel). Arrows indicate borders between early HCC and nontumor tissue. (A) Early HCCs were distinguished from adjacent nontumor tissues by stronger staining of CHC. (B) Early HCCs showed weaker staining of FTCD than adjacent nontumor tissues.

overexpression induces aneuploidy.[14,27] Similarly, the up-regulation of CHC observed in this study might cause chromosome missegregation and lead to HCC development.

FTCD showed strong uniform staining in most nontumor tissue, whereas weak staining was observed in HCC. Interestingly, the intensity of FTCD staining in well-differentiated HCC tissues was more likely to be stronger than that in poorly differentiated HCC tissues, suggesting that the expression of FTCD might be involved in the dedifferentiation of tumor cells. FTCD was previously identified as a 58-kDa rat liver protein with the cytoplasmic surface of the Golgi apparatus *in vivo*.[28] It is considered that FTCD is a liver-specific enzyme that controls folic acid metabolism.[29] Although FTCD has also been recognized as a liver-specific antigen recognized by the sera of patients with autoimmune hepatitis,[30] its involvement in carcinogenesis has not been reported. Thus, our observation is the first report that suggests that down-regulation of FTCD participates in liver carcinogenesis. Further studies are needed to elucidate the precise mechanism of FTCD down-regulation in HCC.

Ku86 is a DNA end-binding molecule that plays an important role in the process of DNA damage signaling and repair, which is thought to maintain genomic stability. Mice deficient in Ku86 showed a marked increase in chromosomal aberrations, and the loss of p53 and Ku86 promotes tumorigenesis, which suggests that Ku86 suppresses tumor development by maintaining the integrity of the genome.[31] Furthermore, recent observation showed that haplo-insufficiency of Ku80 (=Ku86) in poly(ADP-ribose) polymerase-1 (PARP-1)$^{-/-}$ mice promotes the development of hepatocellular adenoma and hepatocellular carcinoma,[32] suggesting that down-regulation of Ku80 is also important for liver carcinogenesis. In contrast, there are some examples in which the up-regulation of Ku86 is associated with tumor progression. Increased expression of Ku70 and Ku86 in a COX-2–dependent mechanism might be associated with hyperproliferation of gastric cancer cells.[33] In addition, increased expression of Ku86 has been reported in B-cell chronic lymphocytic leukemia and in aggressive breast tumors.[34,35] More precise work is needed to examine the expression level of Ku86 in various tumors and to test whether overexpression of Ku86 is a cause or consequence of tumorigenesis.

Rhodanese (EC 2.8.1.1) was originally identified as a mitochondrial matrix enzyme and was proposed to play a role in cyanide detoxification.[36] Recently, it was demonstrated that H_2S is a potent toxin normally present in the colonic lumen, which may play a role in ulcerative colitis, and rhodanese is the principal enzyme involved in H_2S detoxification.[37] In fact, the expression of rhodanese was focally lost in ulcerative colitis.[38] Moreover, rhodanese was markedly reduced in advanced colon cancer.[38] Given that chronic inflammation is an important underlying

condition for tumor development,[39] anti-inflammatory protein such as rhodanese might prevent tumor progression. Recent data have also expanded the concept that inflammation is a critical component of carcinogenesis. In this regard, down-regulation of rhodanese might be a cause of HCC development and could be a potential target for cancer therapy.

Vinculin has a crucial role in the maintenance and regulation of cell adhesion and migration. On recruitment to cell–cell and cell–matrix adherens-type junctions, vinculin becomes activated and mediates various protein–protein interactions that regulate the links between F-actin and the cadherin and integrin families of cell adhesion molecules.[40] Because the loss of cell–cell and cell–matrix interaction is crucial for the development of tumors, down-regulation of vinculin might contribute to carcinogenesis. In fact, the expression of vinculin was repressed in lung carcinoma in surfactant protein C (SP-C)/c-raf transgenic mice.[41] Overexpression of vinculin suppresses tumorigenicity in transformed cells,[42] whereas cancer cells lacking vinculin enhance cell motility and are highly metastatic.[43,44] Our finding that vinculin was repressed in HCC further supports its tumor suppressor function. Interestingly, although full-length vinculin is 117 kDa, smaller molecular weight protein (the major one being 60 kDa) was observed and down-regulated in nontumor tissues. Several reports have shown proteolytic cleavage of vinculin. For example, vinculin is proteolyzed by calpain into at least three fragments (105, 95, 85 kDa[45]) during platelet aggregation. Conversely, alpha-actinin–vinculin interactions causes the conformational change of vinculin and generate an approximately 60-kDa fragment of vinculin by papain treatment[46]; therefore, it is necessary to confirm whether these low molecular proteins are degradation products of vinculin.

In summary, we identified several proteins that are useful to confirm the diagnosis of HCC. They could make significant contributions to the diagnosis of HCC and might also be potential therapeutic targets for cancer control and prevention. Further investigation is needed to uncover the mechanisms responsible for altered protein expressions in HCC.

References

1. Parkin DM, Bray F, Ferlay J, Pisani P. Estimating the world cancer burden: Globocan 2000. Int J Cancer 2001;94:153-156.
2. Feitelson MA, Sun B, Satiroglu Tufan NL, Liu J, Pan J, Lian Z. Genetic mechanisms of hepatocarcinogenesis. Oncogene 2002;21:2593-2604.
3. Pisani P, Parkin DM, Bray F, Ferlay J. Estimates of the worldwide mortality from 25 cancers in 1990. Int J Cancer 1999;83:18-29.
4. Statistics and Information Dept., Minister's Secretariat, Ministry of Health. Vital statistics of Japan 2003. Tokyo, 2003, 66-67.
5. Llovet JM, Burroughs A, Bruix J. Hepatocellular carcinoma. Lancet 2003; 362:1907-1917.
6. Nomura F, Ishijima M, Kuwa K, Tanaka N, Nakai T, Ohnishi K. Serum des-gamma-carboxy prothrombin levels determined by a new generation of sensitive immunoassays in patients with small-sized hepatocellular carcinoma. Am J Gastroenterol 1999;94:650-654.
7. Bruix J, Sherman M. Management of hepatocellular carcinoma. HEPATOLOGY 2005;42:1208-1236.
8. Liang CR, Leow CK, Neo JC, Tan GS, Lo SL, Lim JW, et al. Proteome analysis of human hepatocellular carcinoma tissues by two-dimensional difference gel electrophoresis and mass spectrometry. Proteomics 2005;5: 2258-2271.
9. Lim SO, Park SJ, Kim W, Park SG, Kim HJ, Kim YI, et al. Proteome analysis of hepatocellular carcinoma. Biochem Biophys Res Commun 2002;291:1031-1037.
10. Li C, Hong Y, Tan YX, Zhou H, Ai JH, Li SJ, et al. Accurate qualitative and quantitative proteomic analysis of clinical hepatocellular carcinoma using laser capture microdissection coupled with isotope-coded affinity tag and two-dimensional liquid chromatography mass spectrometry. Mol Cell Proteomics 2004;3:399-409.
11. Santamaria E, Munoz J, Fernandez-Irigoyen J, Prieto J, Corrales FJ. Toward the discovery of new biomarkers of hepatocellular carcinoma by proteomics. Liver Int 2007;27:163-173.
12. Wright LM, Kreikemeier JT, Fimmel CJ. A concise review of serum markers for hepatocellular cancer. Cancer Detect Prev 2007;31:35-44.
13. Oh-Ishi M, Satoh M, Maeda T. Preparative two-dimensional gel electrophoresis with agarose gels in the first dimension for high molecular mass proteins. Electrophoresis 2000;21:1653-1669.
14. Tomonaga T, Matsushita K, Yamaguchi S, Oh-Ishi M, Kodera Y, Maeda T, et al. Identification of altered protein expression and post-translational modifications in primary colorectal cancer by using agarose two-dimensional gel electrophoresis. Clin Cancer Res 2004;10:2007-2014.
15. Nishimori T, Tomonaga T, Matsushita K, Oh-Ishi M, Kodera Y, Maeda T, et al. Proteomic analysis of primary esophageal squamous cell carcinoma reveals downregulation of a cell adhesion protein, periplakin. Proteomics 2006;6:1011-1018.
16. Capurro M, Wanless IR, Sherman M, Deboer G, Shi W, Miyoshi E, et al. Glypican-3: a novel serum and histochemical marker for hepatocellular carcinoma. Gastroenterology 2003;125:89-97.
17. Di Tommaso L, Franchi G, Park YN, Fiamengo B, Destro A, Morenghi E, et al. Diagnostic value of HSP70, glypican 3, and glutamine synthetase in hepatocellular nodules in cirrhosis. HEPATOLOGY 2007;45:725-734.
18. Roncalli M, Roz E, Coggi G, Di Rocco MG, Bossi P, Minola E, et al. The vascular profile of regenerative and dysplastic nodules of the cirrhotic liver: implications for diagnosis and classification. HEPATOLOGY 1999;30:1174-1178.
19. Bosch FX, Ribes J, Diaz M, Cleries R. Primary liver cancer: worldwide incidence and trends. Gastroenterology 2004;127:S5-S16.
20. Stachurski D, Miron PM, Al-Homsi S, Hutchinson L, Lee Harris N, Woda B, et al. Anaplastic lymphoma kinase-positive diffuse large B-cell lymphoma with a complex karyotype and cryptic 3′ ALK gene insertion to chromosome 4 q22–24. Hum Pathol 2007;38:940-945.
21. Argani P, Lui MY, Couturier J, Bouvier R, Fournet JC, Ladanyi M. A novel CLTC-TFE3 gene fusion in pediatric renal adenocarcinoma with t(X;17)(p11.2;q23). Oncogene 2003;22:5374-5378.
22. Chikatsu N, Kojima H, Suzukawa K, Shinagawa A, Nagasawa T, Ozawa H, et al. ALK+, CD30-, CD20- large B-cell lymphoma containing anaplastic lymphoma kinase (ALK) fused to clathrin heavy chain gene (CLTC). Mod Pathol 2003;16:828-832.
23. Ma Z, Hill DA, Collins MH, Morris SW, Sumegi J, Zhou M, et al. Fusion of ALK to the Ran-binding protein 2 (RANBP2) gene in inflammatory myofibroblastic tumor. Genes Chromosomes Cancer 2003;37:98-105.
24. Bridge JA, Kanamori M, Ma Z, Pickering D, Hill DA, Lydiatt W, et al. Fusion of the ALK gene to the clathrin heavy chain gene, CLTC, in inflammatory myofibroblastic tumor. Am J Pathol 2001;159:411-415.
25. Dodge GR, Kovalszky I, McBride OW, Yi HF, Chu ML, Saitta B, et al. Human clathrin heavy chain (CLTC): partial molecular cloning, expression, and mapping of the gene to human chromosome 17q11-qter. Genomics 1991;11:174-178.

26. Royle SJ, Bright NA, Lagnado L. Clathrin is required for the function of the mitotic spindle. Nature 2005;434:1152-1157.
27. Tomonaga T, Matsushita K, Ishibashi M, Nezu M, Shimada H, Ochiai T, et al. Centromere protein H is up-regulated in primary human colorectal cancer and its overexpression induces aneuploidy. Cancer Res 2005;65: 4683-4689.
28. Bloom GS, Brashear TA. A novel 58-kDa protein associates with the Golgi apparatus and microtubules. J Biol Chem 1989;264:16083-16092.
29. Bashour AM, Bloom GS. 58K, a microtubule-binding Golgi protein, is a formiminotransferase cyclodeaminase. J Biol Chem 1998;273:19612-19617.
30. Lapierre P, Hajoui O, Homberg JC, Alvarez F. Formiminotransferase cyclodeaminase is an organ-specific autoantigen recognized by sera of patients with autoimmune hepatitis. Gastroenterology 1999;116:643-649.
31. Difilippantonio MJ, Zhu J, Chen HT, Meffre E, Nussenzweig MC, Max EE, et al. DNA repair protein Ku80 suppresses chromosomal aberrations and malignant transformation. Nature 2000;404:510-514.
32. Tong WM, Cortes U, Hande MP, Ohgaki H, Cavalli LR, Lansdorp PM, et al. Synergistic role of Ku80 and poly(ADP-ribose) polymerase in suppressing chromosomal aberrations and liver cancer formation. Cancer Res 2002;62:6990-6996.
33. Lim JW, Kim H, Kim KH. Expression of Ku70 and Ku80 mediated by NF-kappa B and cyclooxygenase-2 is related to proliferation of human gastric cancer cells. J Biol Chem 2002;277:46093-46100.
34. Klein A, Miera O, Bauer O, Golfier S, Schriever F. Chemosensitivity of B cell chronic lymphocytic leukemia and correlated expression of proteins regulating apoptosis, cell cycle and DNA repair. Leukemia 2000;14:40-46.
35. Pucci S, Mazzarelli P, Rabitti C, Giai M, Gallucci M, Flammia G, et al. Tumor specific modulation of KU70/80 DNA binding activity in breast and bladder human tumor biopsies. Oncogene 2001;20:739-747.
36. Scott EM, Wright RC. Genetic polymorphism of rhodanese from human erythrocytes. Am J Hum Genet 1980;32:112-114.
37. Picton R, Eggo MC, Merrill GA, Langman MJ, Singh S. Mucosal protection against sulphide: importance of the enzyme rhodanese. Gut 2002;50:201-205.
38. Ramasamy S, Singh S, Taniere P, Langman MJ, Eggo MC. Sulfide-detoxifying enzymes in the human colon are decreased in cancer and upregulated in differentiation. Am J Physiol Gastrointest Liver Physiol 2006;291:G288-G296.
39. Coussens LM, Werb Z. Inflammation and cancer. Nature 2002;420:860-867.
40. Bakolitsa C, Cohen DM, Bankston LA, Bobkov AA, Cadwell GW, Jennings L, et al. Structural basis for vinculin activation at sites of cell adhesion. Nature 2004;430:583-586.
41. Rutters H, Zurbig P, Halter R, Borlak J. Towards a lung adenocarcinoma proteome map: studies with SP-C/c-raf transgenic mice. Proteomics 2006; 6:3127-3137.
42. Rodriguez Fernandez JL, Geiger B, Salomon D, Sabanay I, Zoller M, Ben-Ze'ev A. Suppression of tumorigenicity in transformed cells after transfection with vinculin cDNA. J Cell Biol 1992;119:427-438.
43. Raz A, Geiger B. Altered organization of cell-substrate contacts and membrane-associated cytoskeleton in tumor cell variants exhibiting different metastatic capabilities. Cancer Res 1982;42:5183-5190.
44. Coll JL, Ben-Ze'ev A, Ezzell RM, Rodriguez Fernandez JL, Baribault H, Oshima RG, et al. Targeted disruption of vinculin genes in F9 and embryonic stem cells changes cell morphology, adhesion, and locomotion. Proc Natl Acad Sci U S A 1995;92:9161-9165.
45. Serrano K, Devine DV. Vinculin is proteolyzed by calpain during platelet aggregation: 95 kDa cleavage fragment associates with the platelet cytoskeleton. Cell Motil Cytoskeleton 2004;58:242-252.
46. Bois PR, Borgon RA, Vonrhein C, Izard T. Structural dynamics of alpha-actinin-vinculin interactions. Mol Cell Biol 2005;25:6112-6122.

Hepatology Research 2008; **38**: 273–280 doi: 10.1111/j.1872-034X.2007.00259.x

Original Article

Correlation between parametric imaging using contrast ultrasound and the histological differentiation of hepatocellular carcinoma

Katsutoshi Sugimoto,[1] Fuminori Moriyasu,[1] Naohisa Kamiyama,[2] Masahiko Yamada[1] and Hiroko Iijima[3]

[1]*Department of Gastroenterology and Hepatology, Tokyo Medical University, Tokyo,* [2]*The Ultrasound Systems Development Department, Toshiba Medical Systems Corporation, Tochigi and* [3]*Department of Diagnostic Ultrasound, Medical Imaging Center, Hyogo College of Medicine, Hyogo, Japan*

Aim: To determine whether parametric imaging correlates with the degree of histological differentiation of hepatocellular carcinoma (HCC).

Methods: The samples comprised 49 nodules diagnosed histologically as HCC: 19 well differentiated (w-HCC), 22 moderately differentiated (m-HCC), and eight poorly differentiated (p-HCC). The ultrasound (US) equipment used was SSA-770 A (Toshiba Medical Systems, Otawara, Japan) and the contrast agent was SonoVue (Bracco, Milan, Italy). After 1.5 mL of SonoVue was injected intravenously and staining of the tumors and parenchyma was confirmed, microbubbles in the scanned volume were eliminated using high mechanical index (MI) scanning frames. The "arrival time (T_A) images," reflecting β-values, were displayed with color codes at the phase after reperfusion. Images at the phase when the staining reached a plateau (90–180 s) were used as "A images," reflecting A values. These images were compared between each histological grade of differentiation.

Results: Analysis of T_A images indicated that β-values in m-HCC were higher than those in the adjacent non-tumor parenchyma in all 22 samples and also were significantly higher than in the other HCCs ($P < 0.001$ for w-HCC; $P < 0.05$ for p-HCC). Furthermore, β-values in p-HCC samples had significantly larger variations in terms of time and space than in the other HCCs ($P < 0.001$ for w-HCC; $P < 0.01$ for m-HCC). Analysis of A images indicated that the A value for w-HCC was significantly higher than those for either m-HCC or p-HCC ($P < 0.001$).

Conclusion: Both T_A and A images were useful for diagnosing the histological differentiation of HCC.

Key words: contrast-enhanced ultrasound, hepatocellular carcinoma, parametric imaging

INTRODUCTION

HEPATOCELLULAR CARCINOMA (HCC) is the most common primary liver cancer, usually occurring as a complication of chronic liver disease and most often arising in a cirrhotic liver.[1–3] Therefore, accurate surveillance of patients with liver cirrhosis is of great clinical importance because they are at increased risk of HCC.[4] The accurate and early diagnosis of HCC is essential for the treatment of affected patients. Surgical resection, liver transplantation and percutaneous radiofrequency ablation (RFA) are potentially curative therapies for some patients.[5–8]

The histopathologic grades and types of HCC are a well-established prognostic factor.[9,10] It is therefore important to diagnose early and to confirm the type and cellular differentiation before treatment. For many years, fine needle biopsy (FNB) was primarily depended upon to obtain a pathologic diagnosis. However, concerns have been raised about the risk of seeding during FNB aspiration of HCC in patients who will undergo liver transplantation or surgical resection;[11–13] this has been estimated to be up to 3.4%.[14] There are also some reports that have correlated CT and MRI with the histopathologic analysis of HCC.[15,16]

Correspondence: Dr Katsutoshi Sugimoto, Department of Gastroenterology and Hepatology, Tokyo Medical University, 6-7-1 Nishi-Shinjuku, Shinjuku-ku, Tokyo 160-0023, Japan. Email: sugimoto@tokyo-med.ac.jp

Received 28 April 2007; revision 15 July 2007; accepted 22 July 2007.